Electron-impact double ionization of a model helium atom

M. S. Pindzola, D. Mitnik, and F. Robicheaux
Department of Physics, Auburn University, Auburn, Alabama 36849
(Received 11 December 1998)

Single- and double-ionization processes in electron scattering from a model helium atom are calculated by a direct solution of the time-dependent Schrödinger equation on a 3D lattice. The Coulomb interaction between the electrons is described by $v(r_1,r_2)=1/r_>$ and all angular momenta are set to zero. The initial state is a product of the ground state of the model helium atom on a 2D lattice with a wave packet for the free electron. At times following the collision and for incident electron energies around 200 eV, the probability density associated with double ionization is found to be quite small when compared to other scattering processes. Projections onto 1D continuum states are employed to calculate single- and double-ionization cross sections. Although absolute cross sections for the model cannot be compared to experiments on helium due to the neglect of higher partial waves, the ratio of double to single ionization for the model is found to be 1% or less, in fair agreement with experiment. [S1050-2947(99)03806-8]

PACS number(s): 34.80.Dp

I. INTRODUCTION

Substantial progress has been achieved in the last five years in the calculation of accurate electron-impact single-ionization cross sections for atoms and their ions. The correlated quantal dynamics of two free electrons moving in the long-range Coulomb field of a third body remained until this decade one of the most fundamental unsolved problems in nonrelativistic quantum mechanics. The converged close-coupling [1], the hyperspherical close-coupling [2], the *R* matrix with pseudostates [3], and the time-dependent close-coupling [4] methods have all produced direct-ionization cross sections for hydrogen in excellent agreement with experiment [5]. In addition, close-coupling calculations have now been carried out for the direct-ionization cross sections of He [6,7], atomic ions in the Li isoelectronic sequence [8–12], and atomic ions in the Na isoelectronic sequence [13].

In this paper we turn our attention to the calculation of electron-impact double-ionization cross sections for atoms and their ions. The essence of the problem is the description of the correlated quantal dynamics of three free electrons moving in the long-range Coulomb field of a fourth body. To date, fully quantal nonperturbative calculations of the electron-impact double-ionization process have never been reported; in fact, we are not aware of any fully quantal perturbative calculations. In the past various semiempirical and semiclassical approaches have been used to help analyze the many experiments on multiple ionization of atoms and their ions and to predict cross sections of importance to the modeling of high-temperature plasmas [14,15].

We begin by examining the electron-impact double ionization of helium in an *s*-wave model for the Coulomb interaction between the electrons. The full 9D time-dependent Schrodinger equation is reduced to one 3D partial differential equation by setting all angular momenta equal to zero. This same dimensional reduction scheme, or what has come to be known as the Temkin-Poet model [16,17], has proved quite useful in examining the electron-impact single ionization of hydrogen [18–22]. The correlated quantal dynamics found in the *s*-wave model are very similar to those found in the complete physical system. In the following paragraphs we first calculate the single ionization of a model He^+ atomic ion in Sec. II, then calculate the single and double ionization of a model He atom in Sec. III, and finally give a brief summary in Sec. IV.

II. 2D MODEL FOR THE SINGLY CHARGED HELIUM ION

A. Theory

The time-dependent Schrödinger equation for the Temkin-Poet model of He^+ is given by (in atomic units)

$$i\frac{\partial\psi(r_1,r_2,t)}{\partial t}=H(r_1,r_2)\psi(r_1,r_2,t), \tag{1}$$

where the time-independent Hamiltonian is

$$H(r_1,r_2)=-\frac{1}{2}\frac{\partial^2}{\partial r_1^2}-\frac{1}{2}\frac{\partial^2}{\partial r_2^2}-\frac{2}{r_1}-\frac{2}{r_2}+\frac{1}{\max(r_1,r_2)}. \tag{2}$$

The Hamiltonian is discretized on a 2D lattice using lowest-order finite differences. The wave function is then time evolved using an explicit leap-frog propagator [4].

The total antisymmetrized wave function for ^1S scattering from the ground state of He^+ is given by

$$\Psi^{^1S}(r_1,r_2,t)=\sqrt{\frac{1}{2}}[\psi_a(r_1,r_2,t)+\psi_b(r_1,r_2,t)]\times\sqrt{\frac{1}{2}}(\uparrow\downarrow-\downarrow\uparrow), \tag{3}$$

where the arrows represent the two spin degrees of freedom. Initially the spatial wave functions are given by

$$\psi_a(r_1,r_2,t=0)=G_{ks}(r_1)P_{1s}(r_2), \tag{4}$$

and

$$\psi_b(r_1,r_2,t=0)=G_{ks}(r_2)P_{1s}(r_1), \tag{5}$$

where $G_{ks}=[1/(w^2\pi)^{1/4}]e^{[-(r-s)^2/2w^2]}e^{-ikr}$ is an incoming radial wave packet for the free electron, w is the width, s is the localization radius, k is the wave number, and $P_{1s}(r)$ is the ground state of the He^+ ion. We need only time evolve one of the spatial wave functions according to Eq. (1), since the other wave function can be obtained at any time by a simple coordinate interchange.

Following the collision the probability of excitation to a state ns may be extracted from the asymptotic total wave function by the projection:

$$\mathcal{P}^{^1S}_{exc:n}=\int dk' |\langle \chi^{^1S}_{n,k'}(r_1,r_2)|\Psi^{^1S}(r_1,r_2,t=T)\rangle|^2, \tag{6}$$

where

$$\chi^{^1S}_{n,k'}(r_1,r_2)=\sqrt{\frac{1}{2}}[P_{ns}(r_1)\uparrow,P_{k's}(r_2)\downarrow] - \sqrt{\frac{1}{2}}[P_{ns}(r_1)\downarrow,P_{k's}(r_2)\uparrow] \tag{7}$$

and the brackets represent determinants (i.e., $[a(1),b(2)]=a(1)b(2)-a(2)b(1)$). Straightforward reduction yields

$$\mathcal{P}^{^1S}_{exc:n}=2\int dk' \left| \left\langle P_{ns}(r_1)P_{k's}(r_2) \right| \sqrt{\frac{1}{2}}[\psi_a(r_1,r_2,t=T) + \psi_b(r_1,r_2,t=T)] \right\rangle \right|^2. \tag{8}$$

A similar derivation yields the probability of ionization:

$$\mathcal{P}^{^1S}_{ion}=\int dk' \int dk'' \left| \left\langle P_{k's}(r_1)P_{k''s}(r_2) \right| \times \sqrt{\frac{1}{2}}[\psi_a(r_1,r_2,t=T)+\psi_b(r_1,r_2,t=T)] \right\rangle \right|^2. \tag{9}$$

The single-particle orbitals $P(r)$ found in Eqs. (8) and (9) for the excitation and ionization probabilities are obtained by diagonalization of the single-particle Hamiltonian for the He^+ ion:

$$h(r)=-\frac{1}{2}\frac{\partial^2}{\partial r^2}-\frac{2}{r}, \tag{10}$$

on a 1D lattice with the same mesh spacing and box size as the 2D lattice used for Eq. (1). Inelastic cross sections are then given by

$$\sigma=\frac{\pi}{4k^2}(2S+1)\mathcal{P}, \tag{11}$$

where S is the total spin angular momentum.

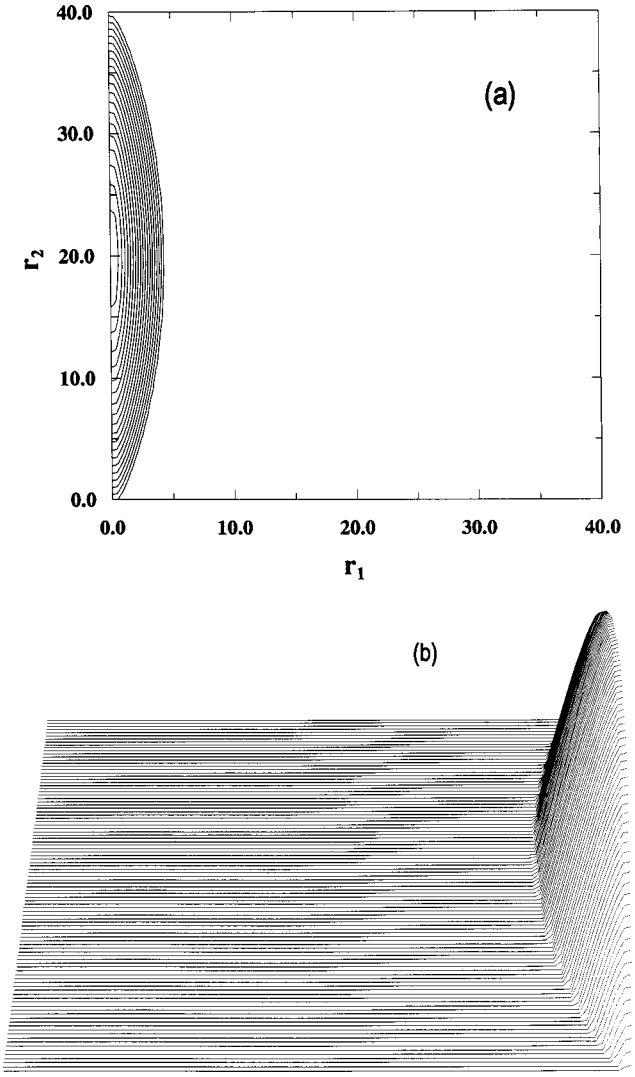

FIG. 1. Initial time ($t=0$) probability density for electron scattering from a model helium ion. (a) 2D contour map and (b) 3D contour projection. (Radial distances are in atomic units.)

B. Results

For electron scattering from He^+ in the Temkin-Poet model we choose a lattice with uniform mesh spacing $\Delta r=0.4$ a.u. and a box size of 40.0 a.u., resulting in a wave-function representation of 10^4 points. Initially the incoming radial wave packet is centered at 20.0 a.u. with a Gaussian full width at half maximum (FWHM) of 6.0 a.u. and an incident electron energy of $E=90$ eV$=3.31$ a.u. The ground state of He^+ on the corresponding 1D lattice was calculated to have an energy of -47.73 eV, the exact analytic value being -54.42 eV. The probability density for the initial unsymmetric spatial wave function, $\psi_b(r_1,r_2,t=0)$, of Eq. (5) is shown in Fig. 1. As time evolves, the peak of the probability density centered at $(r_1=0,r_2=20)$ moves toward the origin with a group velocity of $v=\sqrt{(2E)}=2.57$ a.u.

The time for the wave packet to collapse and then rebound from the origin so that the peak of the elastic-scattering components are centered at $(r_1=0,r_2=20)$ and $(r_1=20,r_2=0)$ is approximately $t=40/v=15.6$ a.u. In Fig. 2 we show the probability density for the unsymmetric spatial wave function, $\psi_b(r_1,r_2,t)$, at $t=20.0$ a.u. The large

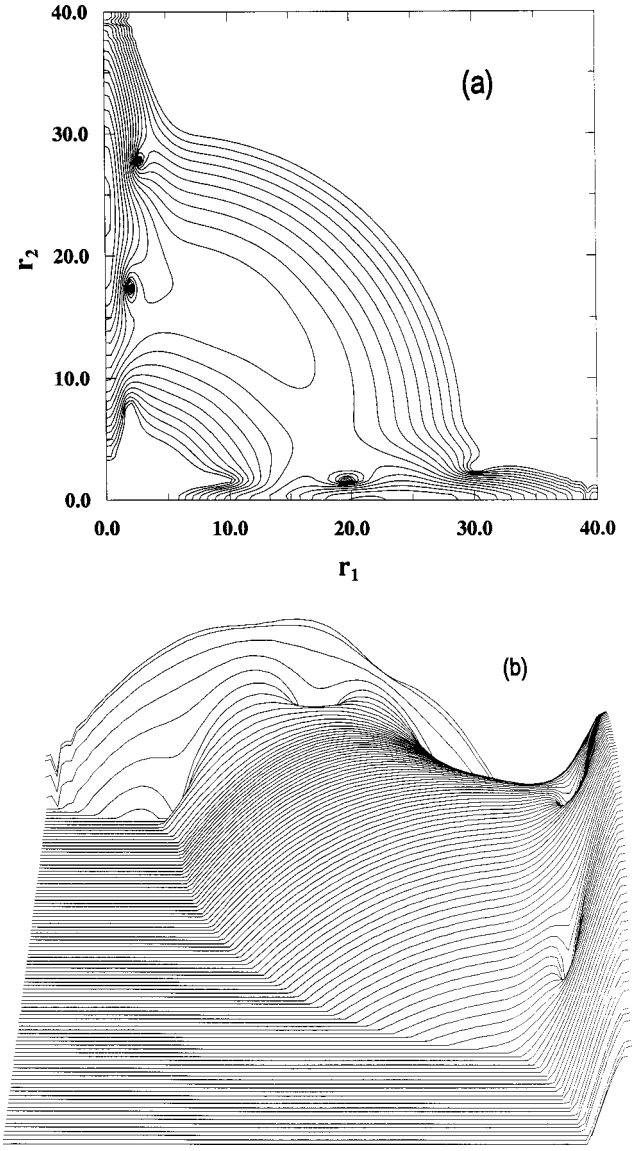

FIG. 2. Final time ($t=20$) probability density for electron scattering from a model helium ion. (a) 2D contour map and (b) 3D contour projection. (Radial distances are in atomic units.)

peaks along the coordinate axes represent elastic and bound inelastic scattering, where one electron remains in the vicinity of the He^+ nucleus at the origin and the other electron moves freely away to large distances. The smaller concentration of probability density along the $r_1=r_2$ axis represents ionization, in which both electrons escape from the He^+ nucleus. In essence, Fig. 2 is a snapshot of the total scattering amplitude, where the distribution in coordinate space may be mapped directly onto a distribution in the momenta of the outgoing electrons for long times.

The probabilities for excitation and ionization of He^+ in the Temkin-Poet model are calculated using Eqs. (8) and (9) at times following the collision (i.e., $T \geqslant 20.0$ a.u.). The time-dependent (TD) 10^4-point-lattice results for the inelastic cross sections are presented in Table I. We repeated the electron-scattering calculations for He^+ using lattices with $\Delta r=0.2$ a.u. and $\Delta r=0.1$ a.u., keeping the box size radius constant at 40.0 a.u. The ground state of He^+ on the corresponding 1D lattice was calculated to have an energy of

TABLE I. Inelastic cross sections for a model helium positive ion at an incident energy of 90 eV (in Mbarns = 1.0×10^{-18} cm^2).

Transition	TD $\Delta r=0.4$	TD $\Delta r=0.2$	TD $\Delta r=0.1$	RMPS [23]
$1s\rightarrow2s$	0.295	0.200	0.173	0.176
$1s\rightarrow3s$	0.080	0.052	0.045	0.044
$1s\rightarrow ks$	0.262	0.172	0.147	0.150

-52.40 eV for $\Delta r=0.2$ a.u. and -53.89 eV for $\Delta r=0.1$ a.u. The 4×10^4-point and 1.6×10^5-lattice results for the inelastic cross sections are also presented in Table I. The $\Delta r=0.1$-a.u. lattice results agree extremely well with the *R*-matrix pseudostate (RMPS) calculations of Bartschat and Bray [23].

As a check on our current numerical procedures we repeated our time-dependent calculations for the excitation and ionization of He^+ using the wave-packet method described in Sec. II of Robicheaux *et al.* [22]. That is, we propagated a fully symmetric spatial wave function, given by $\sqrt{\frac{1}{2}}[\psi_a(r_1,r_2,t)+\psi_b(r_1,r_2,t)]$, and projected the asymptotic solution onto only the negative energy states on the 1D lattice. The excitation probabilities, as well as the ionization probabilities obtained through unitarity, were found to agree exactly with those presented in Table I.

III. 3D MODEL FOR THE HELIUM ATOM

A. Theory

The time-dependent Schrödinger equation for the Temkin-Poet model of He is given by (in atomic units)

$$i\frac{\partial\psi(r_1,r_2,r_3,t)}{\partial t}=H(r_1,r_2,r_3)\psi(r_1,r_2,r_3,t), \quad (12)$$

where the time-independent Hamiltonian is

$$H(r_1,r_2,r_3)=-\frac{1}{2}\frac{\partial^2}{\partial r_1^2}-\frac{1}{2}\frac{\partial^2}{\partial r_2^2}-\frac{1}{2}\frac{\partial^2}{\partial r_3^2}-\frac{2}{r_1}-\frac{2}{r_2}-\frac{2}{r_3}+\frac{1}{\max(r_1,r_2)}+\frac{1}{\max(r_1,r_3)}+\frac{1}{\max(r_2,r_3)}. \quad (13)$$

The Hamiltonian is discretized on a 3D lattice using finite differences and then again time evolved using an explicit leap-frog propagator.

The total antisymmetrized wave function for ^2S scattering from the ground state of He is given by

$$\Psi^{^2S}(r_1,r_2,r_3,t)=\sqrt{\frac{1}{6}}\{[\psi_a(r_1,r_2,r_3,t)-\psi_b(r_1,r_2,r_3,t)]\uparrow\uparrow\downarrow-[\psi_a(r_1,r_2,r_3,t)-\psi_c(r_1,r_2,r_3,t)]\uparrow\downarrow\uparrow+[\psi_b(r_1,r_2,r_3,t)-\psi_c(r_1,r_2,r_3,t)]\downarrow\uparrow\uparrow\}. \quad (14)$$

Initially the spatial wave functions are given by

$$\psi_a(r_1,r_2,r_3,t=0)=G_{ks}(r_1)\phi_{1s^2}(r_2,r_3), \tag{15}$$

$$\psi_b(r_1,r_2,r_3,t=0)=G_{ks}(r_2)\phi_{1s^2}(r_1,r_3), \tag{16}$$

and

$$\psi_c(r_1,r_2,r_3,t=0)=G_{ks}(r_3)\phi_{1s^2}(r_1,r_2), \tag{17}$$

where $\phi_{1s^2}(r,r')$ is the ground state of the He atom. Again we need only time evolve one of the spatial wave functions according to Eq. (12), since the other two can be obtained by coordinate interchange. Since the spatial and spin coordinates cannot be separated in the three-electron problem, we have no choice but to propagate unsymmetric spatial wave functions.

Following the collision the probability of ionization, leaving the He^+ ion in a state ns, may be extracted from the asymptotic total wave function by the projection:

$$\mathcal{P}^{^2S}_{ion:n}=\frac{1}{2}\int dk'\int dk''\left|\left\langle \chi^{(^1S)^2S}_{n,k',k''}(r_1,r_2,r_3)\right.\right. \times\Psi^{^2S}(r_1,r_2,r_3,t=T)\Big\rangle\Big|^2+\frac{1}{2}\int dk'\int dk'' \times\left|\left\langle \chi^{(^3S)^2S}_{n,k',k''}(r_1,r_2,r_3)\right|\Psi^{^2S}(r_1,r_2,r_3,t=T)\right\rangle\right|^2, \tag{18}$$

where

$$\chi^{(^1S)^2S}_{n,k',k''}(r_1,r_2,r_3)=\sqrt{\frac{1}{2}}[P_{ns}(r_1)\uparrow,P_{k's}(r_2)\downarrow,P_{k''s}(r_3)\uparrow] -\sqrt{\frac{1}{2}}[P_{ns}(r_1)\downarrow,P_{k's}(r_2)\uparrow,P_{k''s}(r_3)\uparrow], \tag{19}$$

$$\chi^{(^3S)^2S}_{n,k',k''}(r_1,r_2,r_3)=\sqrt{\frac{2}{3}}[P_{ns}(r_1)\uparrow,P_{k's}(r_2)\uparrow,P_{k''s}(r_3)\downarrow] -\sqrt{\frac{1}{6}}[P_{ns}(r_1)\uparrow,P_{k's}(r_2)\downarrow,P_{k''s}(r_3)\uparrow] -\sqrt{\frac{1}{6}}[P_{ns}(r_1)\downarrow,P_{k's}(r_2)\uparrow,P_{k''s}(r_3)\uparrow], \tag{20}$$

and the brackets represent determinants (i.e., $[a(1),b(2),c(3)]=a(1)b(2)c(3)-a(1)b(3)c(2)-a(2)b(1)c(3)+\cdots$). The factors of $\frac{1}{2}$ in Eq. (18) are needed to avoid double counting in the continuum, while the two terms on the right-hand side of Eq. (18) arise from the spin coupling of the first two electrons in the three electron wave functions. Straightforward but tedious reduction yields

$$\mathcal{P}^{^2S}_{ion:n}=\frac{3}{2}\int dk'\int dk''\left|\left\langle P_{ns}(r_1)P_{k's}(r_2)P_{k''s}(r_3)\right.\right. \times\sqrt{\frac{1}{6}}[2\psi_c(r_1,r_2,r_3,t=T) -\psi_a(r_1,r_2,r_3,t=T)-\psi_b(r_1,r_2,t=T)]\Big\rangle\Big|^2 +\frac{3}{2}\int dk'\int dk''\left|\left\langle P_{ns}(r_1)P_{k's}(r_2)P_{k''s}(r_3)\right.\right. \times\sqrt{\frac{1}{2}}[\psi_a(r_1,r_2,r_3,t=T) -\psi_b(r_1,r_2,r_3,t=T)]\Big\rangle\Big|^2. \tag{21}$$

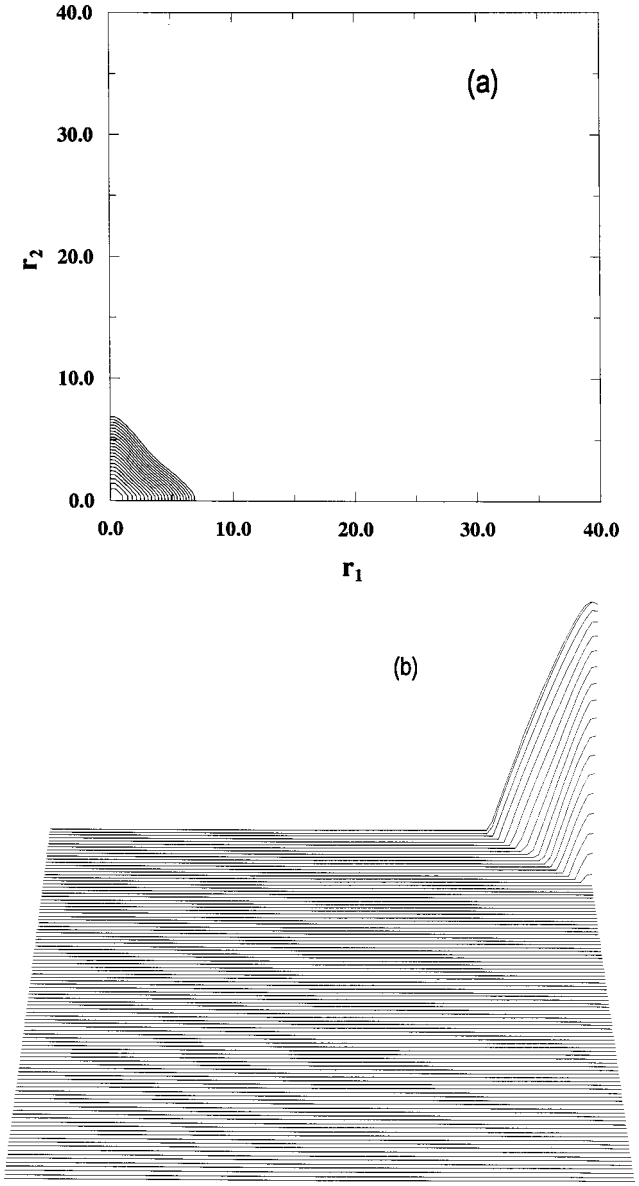

FIG. 3. Probability density for the ground state of a model helium atom. (a) 2D contour map and (b) 3D contour projection. (Radial distances are in atomic units.)

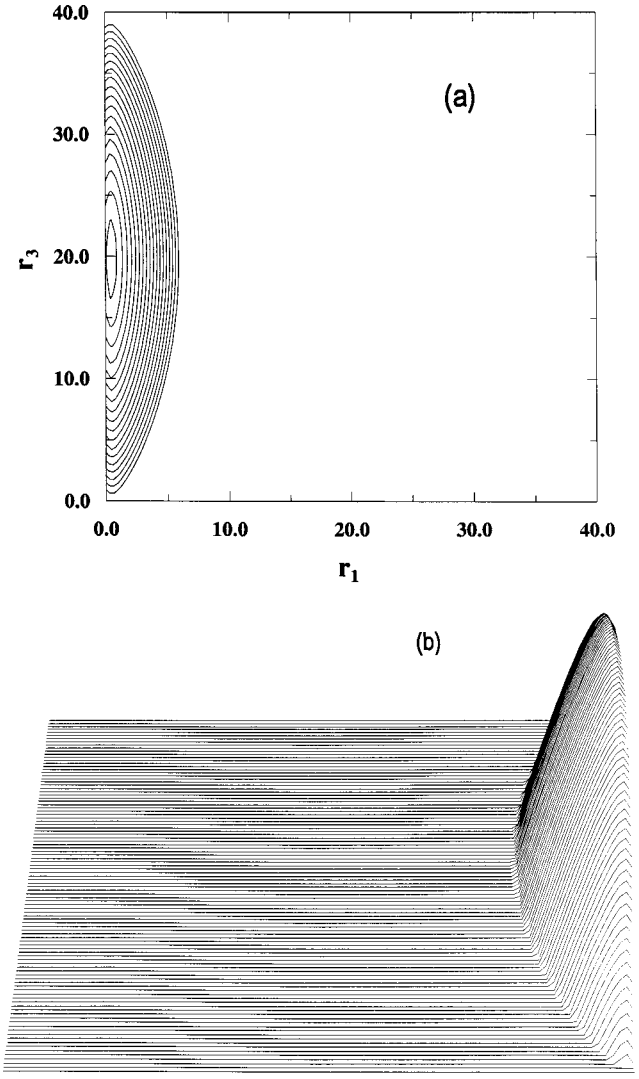

FIG. 4. Initial time ($t=0$) probability density for electron scattering from a model helium atom with $r_2=0$. (a) 2D contour map and (b) 3D contour projection. (Radial distances are in atomic units.)

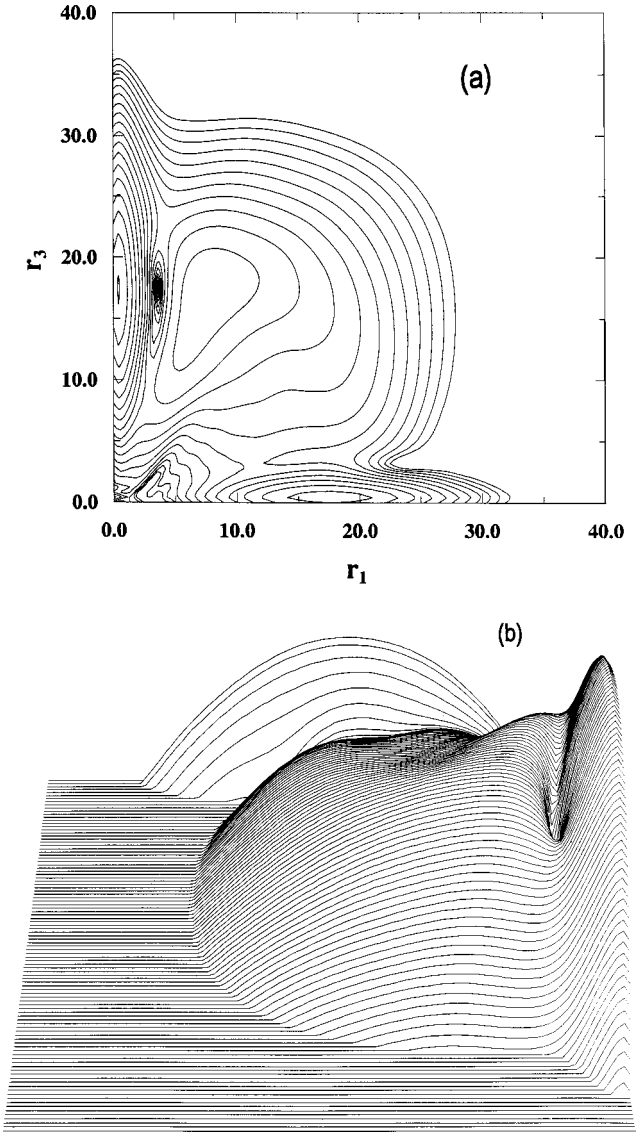

FIG. 5. Final time ($t=15$) probability density for electron scattering from a model helium atom with $r_2=0$. (a) 2D contour map and (b) 3D contour projection. (Radial distances are in atomic units.)

A similar derivation yields the probability of double ionization:

$$\mathcal{P}_{dion}^{^2S}=\frac{1}{2}\int dk'\int dk''\int dk'''\left|\left\langle P_{k's}(r_1)P_{k''s}(r_2)P_{k'''s}(r_3)\right.\right.$$
$$\times\sqrt{\frac{1}{6}}[2\psi_c(r_1,r_2,r_3,t=T)$$
$$\left.\left.-\psi_a(r_1,r_2,r_3,t=T)-\psi_b(r_1,r_2,t=T)]\right\rangle\right|^2$$
$$+\frac{1}{2}\int dk'\int dk''\int dk'''\left|\left\langle P_{k's}(r_1)P_{k''s}(r_2)P_{k'''s}(r_3)\right.\right.$$
$$\times\sqrt{\frac{1}{2}}[\psi_a(r_1,r_2,r_3,t=T)$$
$$\left.\left.-\psi_b(r_1,r_2,r_3,t=T)]\right\rangle\right|^2. \qquad (22)$$

The two-particle wave function, $\phi(r,r')$, for the ground state of the He atom is obtained by imaginary time relaxation of Eq. (1) on a 2D lattice with the same mesh spacing and box size as the 3D lattice used for Eq. (12). The single-particle orbitals, $P(r)$, found in Eqs. (21) and (22) for the single- and double-ionization probabilities are obtained by diagonalization of the Hamiltonian of Eq. (10) on a 1D lattice with the same mesh spacing and box size as the 3D lattice used for Eq. (12). The ionization cross sections are given by Eq. (11), which is simply the probability divided by the incident electron flux.

B. Results

For electron scattering from He in the Temkin-Poet model we choose a lattice with uniform mesh spacing $\Delta r=0.4$ a.u. and a box size of 40.0 a.u., resulting in a wave function representation of 10^6 points. Initially the incoming radial wave packet is centered at 20 a.u. with a Gaussian

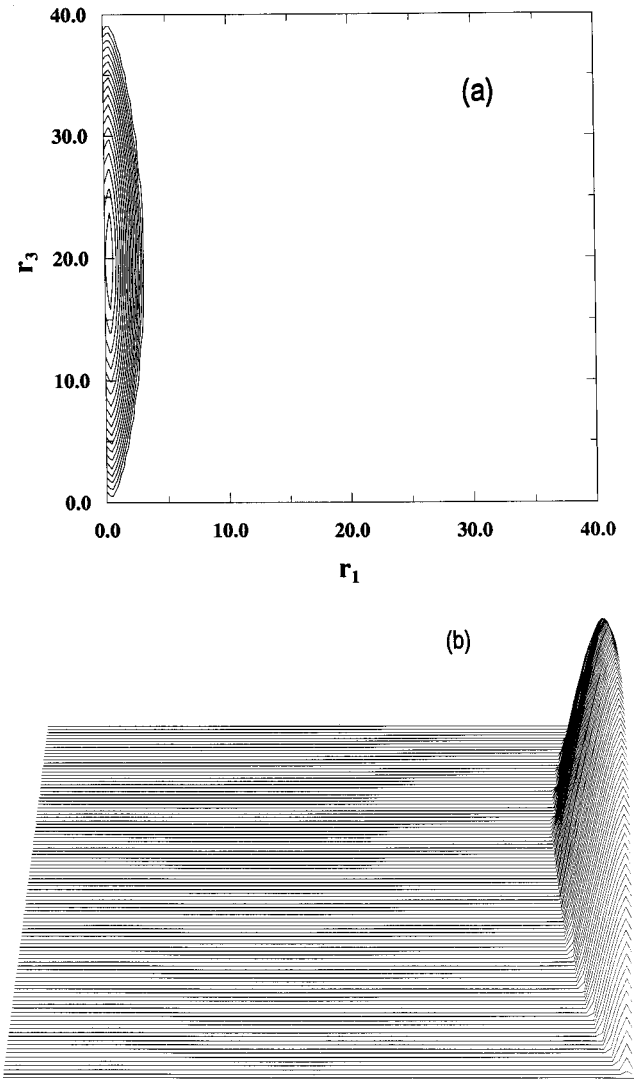

FIG. 6. Initial time ($t=0$) probability density for electron scattering from a model helium atom with $r_2=r_1$. (a) 2D contour map and (b) 3D contour projection. (Radial distances are in atomic units.)

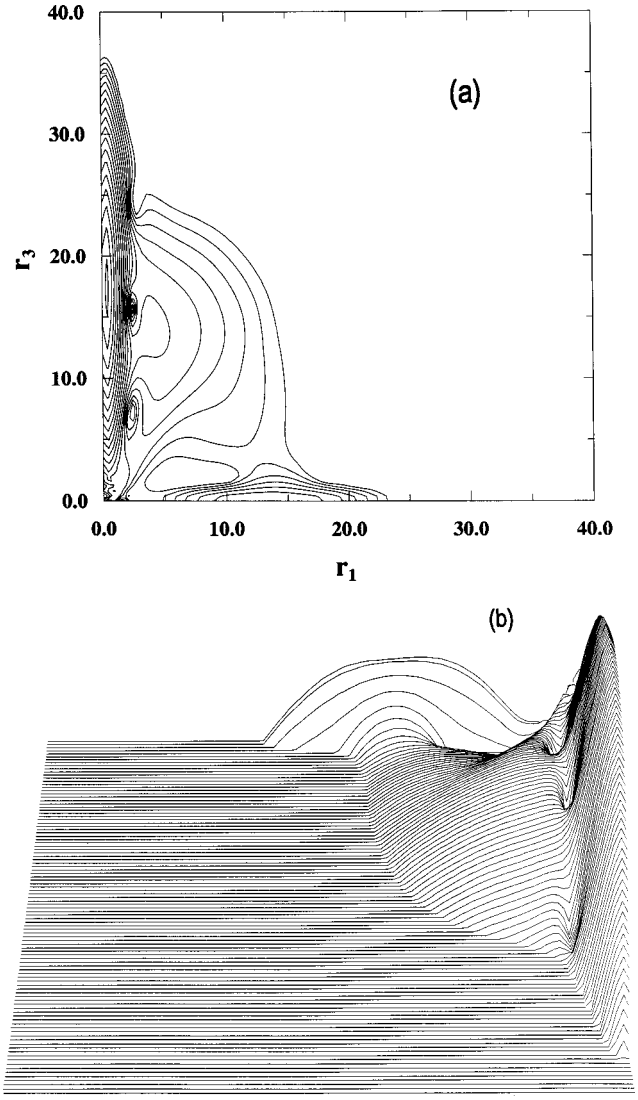

FIG. 7. Final time ($t=15$) probability density for electron scattering from a model helium atom with $r_2=r_1$. (a) 2D contour map and (b) 3D contour projection. (Radial distances are in atomic units.)

FWHM of 6.0 a.u. and an incident electron energy of 200.0 eV. The ground state of He on the corresponding 2D lattice was calculated to have an energy of -67.78 eV. To approach the chemical accuracy for the physical He atom of -79.02 eV would require a smaller lattice spacing and an extension of the model to include higher partial waves (i.e., angular correlations). The probability density for the He ground state wave function, $\phi_{1s^2}(r_1,r_2)$, is shown in Fig. 3. The ''butterfly'' shape of the contour map is due to radial electron correlations.

The visualization of probability flows for a 3D wave function has its challenges. We begin with the probability density for the initial unsymmetric spatial wave function, $\psi_c(r_1,r_2=0,r_3,t=0)$, of Eq. (17) as shown in Fig. 4. In Fig. 5 we show the probability density for $\psi_c(r_1,r_2=0,r_3,t)$ at $t=15.0$ a.u. following the collision. The large peaks along the r_1 and r_3 coordinate axes represent elastic and bound inelastic scattering, where two electrons remain in the vicinity of the He nucleus and the other electron moves away to large distances. Remember $r_2=0$, so one electron is always at the origin. The probability density along the $r_1=r_3$ axis represents single ionization leaving the He^+ ion in a bound state.

To take a look at double ionization, we make a cut along the hyperdiagonal of the coordinate space cube. The probability density of the initial unsymmetric spatial wave function, $\psi_c(r_1,r_2=r_1,r_3,t=0)$, of Eq. (17) is shown in Fig. 6. Notice that the probability density in Fig. 6 along the r_1 axis appears compressed when compared to the probability density found in Fig. 4. This is due to radial correlations in the He atom ground state. As shown in Fig. 3, the probability density extends further along $r_2=0$ than along $r_2=r_1$. In Fig. 7 we show the probability density for $\psi_c(r_1,r_2=r_1,r_3,t)$ at $t=15.0$ a.u. following the collision. The large peak along the r_3 coordinate axis represents elastic and bound inelastic scattering, where two electrons remain in the vicinity of the He nucleus and the third electron moves away to large distances. The smaller peak along the r_1 axis represents single ionization, with only one electron remaining at the origin (remember $r_2=r_1$). Finally the much smaller concentration of probability density along the $r_1=r_2=r_3$ axis

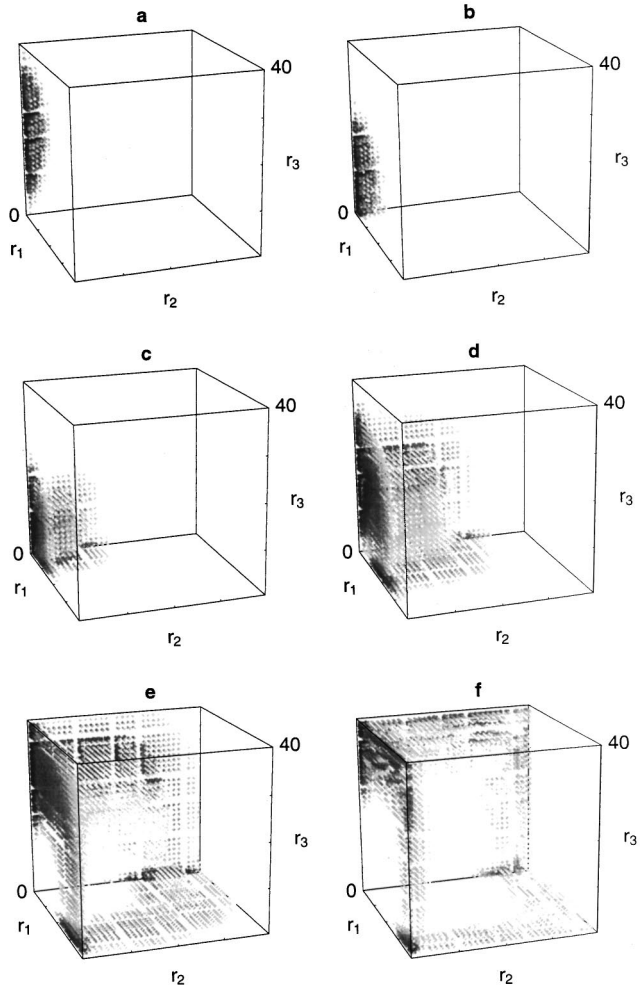

FIG. 8. Time sequence of probability density for electron scattering from a model helium atom at incident energy of 200 eV. (a) $t=0$, (b) $t=5$, (c) $t=10$, (d) $t=15$, (e) $t=20$, and (f) $t=25$. (Radial distances are in atomic units.)

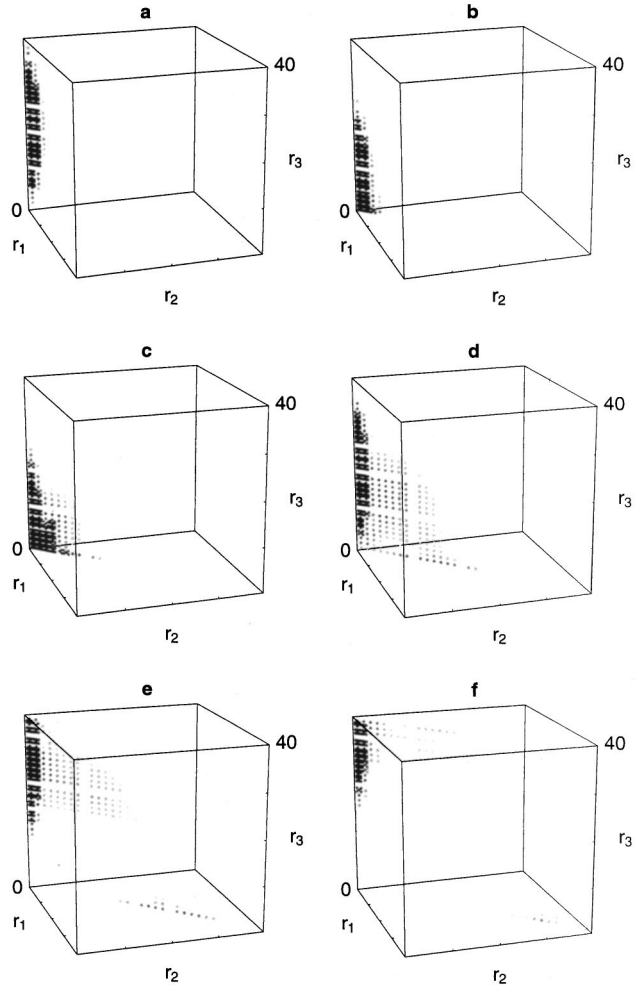

FIG. 9. Time sequence of probability density for electron scattering from a model helium atom at incident energy of 200 eV, at high resolution in only $r_2=r_1$ plane. (a) $t=0$, (b) $t=5$, (c) $t=10$, (d) $t=15$, (e) $t=20$, and (f) $t=25$. (Radial distances are in atomic units.)

represents double ionization, in which all three electrons escape from the nucleus.

We try our hand at 3D probability densities in Figs. 8 and 9. The concentration of points in the dark areas are high density, while light areas are low density. The probability density of the unsymmetric spatial wave function, $\psi_c(r_1,r_2,r_3,t)$, at an incident energy of 200 eV is shown in Fig. 8 for times $t=0.0$, 5.0, 10.0, 15.0, 20.0, and 25.0 a.u. The probability density in the planes (r_2,r_3) and (r_1,r_3) are mirror images of each other and at $t=15.0$ a.u. in Fig. 8(d) correspond with Fig. 5. The low probability density inside the cube represents the time evolution of the three-electron continuum in the Coulomb field of the nucleus. We show the probability density of the unsymmetric spatial wave function, $\psi_c(r_1,r_2,r_3,t)$, only in the plane $(r_1=r_2,r_3)$ in Fig. 9 at the same incident energy and propagation times. Figure 9(d) corresponds with Fig. 7. In this particular plane the probability density inside the cube again represents the time evolution of the electron-impact double-ionization process.

The probabilities for single and double ionization of He in the Temkin-Poet model are calculated using Eqs. (21) and (22) at times following the collision (i.e., $T\geqslant 15.0$ a.u.). The 10^6-point-lattice results for the ionization cross sections are presented in Table II at incident energies of 200, 300, 400, and 500 eV. It is interesting to compare the model He-atom theoretical predictions with the physical He-atom experimental measurements of Shah *et al.* [24], at least at the qualitative level. The peak of the double-ionization cross section in both theory and experiment is between 300 and 400 eV, around 4.4×10^{-21} cm^2 for the model and around 1.3×10^{-19} cm^2 for observation. Of course, the difference in absolute cross section is to be expected since the model does

TABLE II. Ionization cross sections for a model helium atom (asymptotic continuum charge = 2) at a mesh spacing of $\Delta r=0.4$ (in Mbarns = 1.0×10^{-18} cm^2).

Transition	TD $E=200$ eV	TD $E=300$ eV	TD $E=400$ eV	TD $E=500$ eV
$1s^2\rightarrow 1sks$	0.4162	0.2950	0.2232	0.1398
$1s^2\rightarrow 2sks$	0.0207	0.0200	0.0169	0.0111
$1s^2\rightarrow 3sks$	0.0026	0.0028	0.0026	0.0018
$1s^2\rightarrow ksk's$	0.0033	0.0043	0.0044	0.0033

TABLE III. Ionization cross sections for a model helium atom (asymptotic continuum charge = 1) at a mesh spacing of $\Delta r = 0.4$ (in Mbarns = 1.0×10^{-18} cm^2).

Transition	TD $E = 200$ eV	TD $E = 300$ eV	TD $E = 400$ eV	TD $E = 500$ eV
$1s^2 \rightarrow 1sks$	0.7394	0.5155	0.3984	0.2597
$1s^2 \rightarrow 2sks$	0.0622	0.0497	0.0509	0.0518
$1s^2 \rightarrow 3sks$	0.0195	0.0134	0.0094	0.0072

not include the higher partial waves. The ratio of the double- to single-ionization cross sections between 200 and 500 eV varies from 0.8% to 2.2% for the model and from 0.3% to 0.6% for observation.

We further investigated a couple of possibilities for the model's rather large double- to single-ionization cross section ratio. As shown in Sec. II, full convergence of the ionization cross sections for the Temkin-Poet model would require a mesh spacing of $\Delta r = 0.1$ a.u. and a 6.4×10^7 point lattice. However, we note from Table I that the ratio of the ionization to excitation cross sections for He^+ varies quite slowly with mesh spacing. We would expect a similar slow variation for the ratio of double- to single-ionization cross sections for He. A more likely explanation for the model's rather large cross-section ratio may be the choice of single-particle orbitals, $P(r)$, used in the projections found in Eqs. (21) and (22). Certainly the choice of an effective charge of 2 in Eq. (10) is correct for the double-ionization probability of Eq. (22), where all three electrons are escaping to large distances and see a bare He nucleus. However, the choice of an effective charge of 1 in Eq. (10) for the calculation of the two continuum orbitals, $P_{k's}(r)$ and $P_{k''s}(r)$, seems more appropriate for the single-ionization probability of Eq. (21). In single ionization the remaining bound electron should shield the bare He nucleus from the two electrons that are escaping to large distances. The 10^6-point-lattice results for the single-ionization cross sections using an effective charge of 1 for the continuum orbitals, are presented in Table III at incident energies of 200, 300, 400, and 500 eV. The cross sections for $1s$ single ionization are approximately 80% larger than the previous results. With the new single-ionization values, the ratio of the double- to single-ionization cross sections between 200 and 500 eV varies from 0.4% to 1.0%, in much better agreement with observation.

IV. SUMMARY

We have carried out fully quantal nonperturbative calculations for the electron-impact double ionization of helium within an s-wave model of the electron interactions. The numerical method is based on the direct solution of the time-dependent Schrodinger equation on a 3D lattice. Visualization of the wave-packet probability density as a function of time confirms the hierarchy of scattering processes: strong elastic and bound inelastic, weaker single ionization, and extremely weak double ionization. Various ionization cross sections for helium were calculated by time propagation of an unsymmetric spatial wave function, coordinate interchange to recover the remaining parts of the total wave function, and direct projection onto a mixture of bound and continuum single-particle orbitals. The ratios of double to single ionization for the s-wave model were found to be in reasonable agreement with experiments on the physical atom. It should be possible to extend the three-electron wave-packet method to include higher angular waves, resulting in time-dependent close-coupling equations for the total ^2S and ^2P symmetries. Accurate checks could then be made on theoretical predictions [25,26] and experimental measurements [27] of the complete photofragmentation of the lithium atom.

ACKNOWLEDGMENTS

This work was supported in part by a NSF grant (No. PHY-9122199), a NSF young investigator grant (No. PHY-9457903), and a U.S. DOE EPSCoR grant (No. FC02-91ER75678) with Auburn University. The computational work was carried out at the National Energy Research Supercomputer Center in Berkeley, California.

[1] I. Bray and A. T. Stelbovics, Phys. Rev. Lett. **70**, 746 (1993).
[2] D. Kato and S. Watanabe, Phys. Rev. Lett. **74**, 2443 (1995).
[3] K. Bartschat and I. Bray, J. Phys. B **29**, L577 (1996).
[4] M. S. Pindzola and F. Robicheaux, Phys. Rev. A **53**, 1525 (1996).
[5] M. B. Shah, D. S. Elliot, and H. B. Gilbody, J. Phys. B **20**, 3501 (1987).
[6] D. V. Fursa and I. Bray, Phys. Rev. A **52**, 1279 (1995).
[7] E. T. Hudson, K. Bartschat, M. P. Scott, P. G. Burke, and V. M. Burke, J. Phys. B **29**, 5513 (1996).
[8] I. Bray, J. Phys. B **28**, L247 (1995).
[9] K. Bartschat and I. Bray, Phys. Rev. B **30**, L109 (1997).
[10] M. S. Pindzola, F. Robicheaux, N. R. Badnell, and T. W. Gorczyca, Phys. Rev. A **56**, 1994 (1997).
[11] K. Berrington, J. Pelan, and L. Quigley, J. Phys. B **30**, 4973 (1997).
[12] P. J. Marchalant, K. Bartschat, and I. Bray, J. Phys. B **30**, L435 (1997).
[13] N. R. Badnell, M. S. Pindzola, I. Bray, and D. C. Griffin, J. Phys. B **31**, 911 (1998).
[14] H. Deutsch, K. Becker, and T. D. Mark, J. Phys. B **29**, L497 (1996).
[15] *Electron Impact Ionization*, edited by T. D. Mark and G. H. Dunn (Springer-Verlag, Berlin, 1985).
[16] A. Temkin, Phys. Rev. **126**, 130 (1962).
[17] R. Poet, J. Phys. B **11**, 3081 (1978).
[18] J. Callaway and D. H. Oza, Phys. Rev. A **29**, 2416 (1984).
[19] K. W. Meyer, C. H. Greene, and I. Bray, Phys. Rev. A **52**, 1334 (1995).
[20] W. Ihra, M. Draeger, G. Handke, and H. Friedrich, Phys. Rev. A **52**, 3752 (1995).
[21] K. Bartschat and I. Bray, Phys. Rev. A **54**, R1002 (1996).

[22] F. Robicheaux, M. S. Pindzola, and D. R. Plante, Phys. Rev. A **55**, 3573 (1997).
[23] K. Bartschat and I. Bray, Phys. Rev. A **55**, 3236 (1997).
[24] M. B. Shah, D. S. Elliott, P. McCallion, and H. B. Gilbody, J. Phys. B **21**, 2751 (1988).
[25] A. W. Malcherek, J. M. Rost, and J. S. Briggs, Phys. Rev. A **55**, R3979 (1997).
[26] H. W. van der Hart and C. H. Greene, Phys. Rev. Lett. **81**, 4333 (1998).
[27] R. Wehlitz, M. T. Huang, B. D. DePaola, J. C. Levin, I. A. Sellin, T. Nagata, J. W. Cooper, and Y. Azuma, Phys. Rev. Lett. **81**, 1813 (1998).